Direct measurements of luminal Ca^{2+} with endo-lysosomal GFP-aequorin (ELGA) reveal functional IP_3 receptors

Calvo B[1*], Torres-Vidal P[1*], Delrio-Lorenzo A[2], Rodriguez C[1], Aulestia FJ[3], Rojo-Ruiz J[1], Garcia-Sancho J[1], Patel S[4**] and Alonso MT[1**]

[1] Unidad de Excelencia, Instituto de Biomedicina y Genética Molecular de Valladolid (IBGM), Universidad de Valladolid y Consejo Superior de Investigaciones Científicas (CSIC), C/ Sanz y Forés 3, 47003 Valladolid, Spain

[2] Present address: Universidad Alfonso X el Sabio, Madrid. Av. Universidad 1, 28691 Villanueva de la Cañada, Madrid

[3] Present address: Cellus Biomédica, Parque Tecnológico de León, C/ Julia Morros s/n, 24009, León, Spain

[4] Department of Cell and Developmental Biology, University College London, Gower Street, London WC1E 6BT, UK.

* These authors contributed equally to this work

** Corresponding authors: talonso@uva.es and patel.s@ucl.ac.uk

KEYWORDS:

Endo-lysosome, calcium, calcium signalling, aequorin, genetically encoded calcium indicator, acidic organelle, IP3R, calcium release

ABSTRACT

Endo-lysosomes are considered acidic Ca^{2+} stores but direct measurements of luminal Ca^{2+} within them are limited. Here we report that the Ca^{2+}-sensitive luminescent protein aequorin does not reconstitute with its cofactor at highly acidic pH but that a significant fraction of the probe is functional within a mildly acidic compartment when targeted to the endo-lysosomal system. We leveraged this probe (ELGA) to report Ca^{2+} dynamics in this compartment. We show that Ca^{2+} uptake is ATP-dependent and sensitive to blockers of endoplasmic reticulum Ca^{2+} pumps. We find that the Ca^{2+} mobilizing messenger IP_3 which typically targets the endoplasmic reticulum evokes robust luminal responses in wild type cells, but not in IP_3 receptor knock-out cells. Responses were comparable to those evoked by activation of the endo-lysosomal ion channel TRPML1. Stimulation with IP_3-forming agonists also mobilized the store in intact cells. Our data reveal a physiologically-relevant, IP_3-sensitive store of Ca^{2+} within the endo-lysosomal system.

INTRODUCTION

Endo-lysosomes (EL) have emerged as relevant players in subcellular calcium signalling alongside the better characterised endoplasmic reticulum (ER) (Morgan et al., 2011; Patel and Docampo, 2010; Yang et al., 2019). Endo-lysosomal Ca^{2+} has been implicated in most of these organelle functions, such as late endosome-lysosome fusion, lysosomal exocytosis, or membrane repair. Impaired Ca^{2+} signalling can cause defects in the endo-lysosomal trafficking and eventually can provoke lysosome storage diseases (LSDs). These so called acidic Ca^{2+} stores are thought to accumulate high amounts of Ca^{2+} (in the range of 0.4-0.6 mM, similar to the endoplasmic reticulum (ER) (Christensen et al., 2002; Lloyd-Evans et al., 2008). Akin to ER-localised receptor/Ca^{2+} channels for the second messenger IP_3 which mediate Ca^{2+} release in response to IP_3-forming hormones, various Ca^{2+}-permeable channels have been shown to localize to membranes of late endosome and lysosome. These include Mucolipin transient receptor potential (TRPML1) channels, two pore channels (TPCs) and P_2X_4 channels. TRPML1 is an ubiquitously expressed channel specifically activated by phosphatidylinositol 3,5-bisphosphate ($PI(3,5)P_2$), a low abundant phosphoinositide enriched in endomembranes, and which is mutated in type IV mucolipidosis (Dong et al., 2010).

The ER accumulates Ca^{2+} via SERCA. In contrast, the mechanism responsible for endo-lysosomal Ca^{2+} uptake has not been yet fully elucidated, mainly because of the technical difficulties associated to measure intraluminal Ca^{2+} in an acidic compartment. It is assumed that the vacuolar-type ATPase (V-ATPase) which is present in the endo-lysosome membrane and maintains the proton gradient, drives Ca^{2+} into the lysosomal lumen via a type of transporter of H^+ for Ca^{2+} similar to the Ca^{2+}/H^+ exchanger present in yeast and in some animals (Melchionda et al., 2016; Mindell, 2012). This view has been recently challenged by the proposal that the ER, not the pH gradient, through IP_3R tunnels Ca^{2+} into the endo-lysosomes (Atakpa et al., 2019; Garrity et al., 2016).

Indirect monitoring of cytosolic Ca^{2+} using conventional organic Ca^{2+} dyes (Kilpatrick et al., 2016) or genetic Ca^{2+} indicators targeted to the cytosolic site of the endo-lysosome has provided qualitative insights into Ca^{2+} release channels (Shen et al., 2012). However, direct measurements of luminal Ca^{2+} of the endo-lysosome have been challenging due to the highly acidic pH which interferes with Ca^{2+} binding and

thus requires careful calibration. In this study, we report the use of the Ca^{2+}-sensitive luminescent protein aequorin targeted to the endo-lysosome. In general, aequorin is considered less sensitive to acidic pH than fluorescent genetically encoded Ca^{2+} indicators (Johnson and Shimomura, 1978; Shimomura et al., 1974).

Surprisingly, we find that aequorin does not reconstitute well at extreme acidic pH and therefore reports Ca^{2+} in a mildly acidic compartment of the endo-lysosomal system. We show that this compartment accumulates Ca^{2+} via active uptake and releases it via endogenous IP_3 receptors. Our data extend the actions of IP_3 to the endo-lysosomal system.

RESULTS

ELGA as a novel endo-lysosome Ca indicator

We recently introduced genetically encoded Ca^{2+} indicators based on aequorin fused to GFP (Rodriguez-Garcia et al., 2014; Rodriguez-Prados et al., 2015). Here, we targeted them to the endo-lysosomal system by fusing the N-terminal of GFP-aequorin (GA) to the C-terminal of the tetanus-insensitive vesicle-associated membrane protein (VAMP7), a marker of the late endosomes and secretory lysosome (Pryor et al., 2004; Vats and Galli, 2022) (***Figure 1A***). VAMP-7 is composed of a cytosolic region, an endo-lysosomal transmembrane domain and a luminal C-terminal domain. Therefore, the Ca^{2+} indicators are expected to be confined into the endo-lysosomal lumen (***Figure 1B***). Due to the expected high endo-lysosomal luminal Ca^{2+}, we introduced the D119A mutation in aequorin to lower the affinity for Ca^{2+}. This probe was dubbed ELGA (for Endo-Lysosomal GFP-Aequorin). We generated a second variant (ELGA1) with additional substitutions (D117A, and D163A) to further reduce the affinity, lowering rate of aequorin consumption and thereby allowing longer recordings (up to ~1h). Note that GA1 was a variant previously published as GAP1 (Rodriguez-Garcia et al., 2014; Rodriguez-Prados et al., 2015) but renamed here to maintain a comprehensive nomenclature. Both probes can measure Ca^{2+} in the range of 100-1000 μM (***Figure 1 – figure supplement 1A***). The Ca^{2+} sensors were expressed (either transiently or stably) in mammalian cells using a relatively weak herpes simplex virus type 1 (HSV-1)

promoter (Geller, 1991), to limit the amount of expressed protein and, hence, to minimize mistargeting.

As shown in ***Figure 1C- supplement movie 1)***, ELGA and ELGA1 both localized to punctate structures. To characterize the subcellular distribution of the ELGAs we performed colocalization analysis with various endogenous organellar markers. ***Figure 1D*** shows representative confocal images of HEK293T cells transfected with ELGA and fixed one day later. The endogenous lysosome-associated membrane protein 2 (LAMP-2) was assayed by immunodetection with a specific antibody (***Figure 1D***). There was colocalization of ELGA with LAMP2, whereas there was no significant overlap with markers for other organelles such as ER, early endosome, or mitochondria (***Figure 1D and supplement Table 1***). Altogether, these results indicate that the majority of the ELGA indicator is localized to a subset of endo-lysosomes.

ELGA reports Ca^{2+} in mildly acidic compartments

To analyse the ability of aequorin to report Ca^{2+} at acidic pHs, we compared the maximal luminescence signal triggered by Ca^{2+} in the range from 4.5 up to 7.2 pH. Recombinant GA regenerated with coelenterazine showed maximal luminescence activity at 7.2 pH that decreased proportionally at lower pHs (6.5 and 6.0 pH) up to a threshold of 5.5 pH, below which the Ca^{2+} sensor was not functional (***Figure 1E).*** Similar results were obtained with GA1 or with the original aequorin, either reconstituted with native coelenterazine or with its lower affinity *n* analogue (***Figure supplement 2***), indicating that the effect of acidic pH on the luminescent function is independent on the affinity of aequorin for Ca^{2+}. This was surprising, given previous calibration/performance studies at acidic pH (Mitchell et al., 2001; Ronco et al., 2015; SantoDomingo et al., 2010). If the aequorin-based Ca^{2+} sensor was first reconstituted at neutral (7.2) and then, shifted to 4.5 pH for the luminescence assay, the luminescence activity was recovered, suggesting that the lack of light emission is due to the binding of the cofactor to apoaequorin (***Figure 1F)***.

The above findings precluded measurement of Ca^{2+} at highly acidic pH such as that found in lysosomes. But because the pH of endocytic organelles is diverse (e.g., early endosome, pH 6.5; late endosomes, pH 6.0; lysosome, pH 4.5), we reasoned that ELGAs could be used to report Ca^{2+} in less acidic compartments within the EL

system. To determine whether ELGAs reside in such compartments, we leveraged the pH sensitivity of the GFP moiety in ELGA. GFP fluorescence is quenched at acidic pH (pKa ~6). Thus, any detectable GFP fluorescence in live cells should reflect targeting to a compartment with a pH>5 within the range where aequorin can be reconstituted. As shown in ***Figure 1G***, punctate GFP fluorescence was readily detectable in live HeLa and HEK293 cells, both transfected with ELGA.

To assess the properties of the probes at less acidic pH, we performed Ca^{2+} calibrations at pH 7.2 and 6. Essentially similar values were obtained at both pH values, indicating no major effect within this range. As shown in ***Figure 1H-supplement 1A***, the affinity of GA1 for Ca^{2+} was ~350 μM at pH 7.2.

Taken together, these results identify ELGAs as reporters of Ca^{2+} within mildly acidic compartments.

Uptake of Ca^{2+} is ATP-dependent and sensitive to blockers of SERCA

In order to directly monitor uptake and exit of Ca^{2+} within the endo-lysosomal compartment, we used digitonin-permeabilized HEK293T cells expressing ELGA1 perfused with a cytosol-like solution. As we expected the endo-lysosome to be a high Ca^{2+} content store, it needed to be depleted of Ca^{2+} before aequorin was regenerated with its cofactor to avoid its premature consumption. But the mechanisms of store filling are unclear. We first tested Bafilomycin A1 prior to adding the coelenterazine: this compound inhibits the V-type ATPase and has been used widely to disrupt the activity of putative Ca^{2+}-H^{+} exchangers. Bafilomycin A1 treatment did not produce a measurable luminescent signal (data not shown), indicating that aequorin had been consumed likely because the target store was not emptied of Ca^{2+}. These data are consistent with functional targeting of ELGA to a non-highly acidic compartment.

By contrast, incubation with the reversible SERCA inhibitor tert-butylhydroquinone (tBHQ), produced a robust luminescence with a good signal to noise ratio (***Figure 2A***). Under these conditions perfusion with cytosol-like medium (free $[Ca^{2+}]$ = 200 nM) initiated Ca^{2+} uptake at a rate of 8 ± 0.6 μM/s (n=36), reaching a value of $[Ca^{2+}]_{EL}$ at the steady-state of 365 ± 21 μM (n=54) in 3 ± 0.6 min (n=7) (***Figure 2A and B***). Other cell types tested, e.g., HeLa, CHO or MDCK cells displayed similar responses (***Figure 2B- figure supplement 3).*** We tested the effect of Bafilomycin A1.

Bafilomycin A1 (1 μM) added acutely or following incubation for 1 h had little effect on the $[Ca^{2+}]_{EL}$(***Figure supplement 4***), consistent with the failure to reconstitute the probe in its presence.

Ca^{2+} uptake was ATP-dependent because there was little change in luminescence in the absence of ATP (90 ± 4% inhibition, n=7; ***Figure 2C and F- figure supplement 1B-C*)**. Similarly, the SERCA specific inhibitors thapsigargin or tBHQ provoked a complete inhibition of the EL Ca^{2+} uptake (98 ± 1%, n=7; and 97 ± 2%, n=8; ***Figure 2D and E,*** respectively). In this last case, washing out of the reversible inhibitor rapidly restored the Ca^{2+} uptake up to normal rate (***Figure 2E and F***). Once the endo-lysosomal lumen is fully replenished with Ca^{2+}, its removal (addition of 0.1 mM EGTA) caused a progressive and complete decline in the $[Ca^{2+}]_{EL}$ at a rate of ~2.0 μM/s (***Figure 2G)***. Likewise, removal of ATP or application of tBHQ, either in the presence or absence of Ca^{2+}, emptied the EL-Ca^{2+} store. Statistical quantifications of the EL-Ca^{2+}-exit rate are shown in ***Figure 2H.***

Collectively, these results indicate that the endo-lysosome can accumulate high amounts of Ca^{2+} through a SERCA mechanism.

IP_3 mobilizes Ca^{2+} from endo-lysosomal Ca^{2+} stores

To explore endogenous Ca^{2+} release pathways, we examined the effect of NAADP, which activates endo-lysosomal TPCs. NAADP evoked a fast reversible response that released 30% of the EL-Ca^{2+} content, both in HEK and HeLa cells. But the responses were inconsistent and observable in around ~ 50% of trials (***Figure supplement 5***). Surprisingly, addition of IP_3 (2 μM, 30s) produced a fast and strong Ca^{2+} release from the endo-lysosomal store that reduced the endo-lysosomal luminal $[Ca^{2+}]_{EL}$ by 72.56 ± 1.41 % (n= 18) **(*Figure 3A and 3F*)**. The IP_3 release was very robust and consistent in all cell types tested (HeLa, CHO or MDCK cells; representative results are shown in ***figure supplement 6***). This effect was concentration dependent, from 0.01 μM, that produced a small but detectable effect, up to 10 μM, a maximum effect, comparable to that with 30 μM, the highest IP_3 concentration tested **(*Figure 3B,*** and summary data in ***Figure 3C*)**.

To test specificity of the IP_3 response, we used IP_3R-null HEK293 (HEK-3KO) cell line generated by CRISPR/Cas9 technology (Alzayady et al., 2016). As shown in ***Figure 3D***, IP_3-induced Ca^{2+} release was abrogated (1.36 ± 0.97 % (n= 12).

Interestingly, in these cells both the EL-Ca^{2+} refilling rate (6.7 ± 0.7 μM/s) and the $[Ca^{2+}]_{EL}$ reached at the steady-state (369 ± 32 μM; n= 12) coincided with those values obtained in IP_3 replete control cells for resting $[Ca^{2+}]_{EL}$ (365 ± 21 μM; n= 54) and for Ca^{2+} refilling rate (8.0 ± 0.6 μM/s (n= 36) (***figure supplement 7)***. This suggests that, unless there are compensatory effects, IP_3R is not essential for refilling EL-Ca^{2+} store. We also examined the effect of IP_3 in HEK-3KO cells upon re-expression of IP_3R1. As shown in ***Figure 3E and F***, the IP_3 response was partially rescued (54.44 ± 1.20 %; n= 7)**.**

In an independent approach, we used heparin, an inhibitor of the IP_3R. Heparin completely blocked the IP_3 response (92 ± 2 % inhibition; n= 5; ***Figure 3G and 3H***). Collectively, both genetic and pharmacological approaches reveal the presence of functional IP_3Rs within the endo-lysosomal Ca^{2+} store that support robust luminal Ca^{2+} responses.

ELGA responses are independent of the ER

Because of the similarities in the properties of the Ca^{2+} stores reported by ELGA and the ER with respect to both Ca^{2+} uptake and Ca^{2+} release, we considered the possibility that a fraction of the probe may be mistargeted to the ER.

To address this, we expressed TRPML1, a major endo-lysosomal Ca^{2+} channel. Colocalization analysis of ELGA with TRPML in fixed cells is shown in ***Figure 4A***. Both probes were targeted to the same compartment. Colocalization significantly decreased in live cells (***Figures 4A and B***) indicating that a proportion of ELGA is located to acidic, non-fluorescent vesicles in live cells that become fluorescent when the pH increases upon fixation. These results are consistent with ELGA as a Ca^{2+} reporter in a fraction of the endo-lysosomal system.

Interestingly, TRPML1 expression drastically reduced the levels of Ca^{2+} reported by ELGA1 (***Figure 4C)***. In contrast, Ca^{2+} levels in the ER measured using the same reporter targeted to the ER were unchanged upon TRPML1 expression, indicating that the channel is specifically leaky in the endo-lysosomal store. These functional data distinguish EL and ER Ca^{2+} stores. In accord, there was no correlation between EL and ER Ca^{2+} levels in the cell types used (***Figure 4D).***

To further explore the properties of TRPML1, we activated it with the specific membrane-permeable synthetic agonist ML-SA1. In transiently expressing TRPML1 HEK293T cells, ML-SA1 (20 μM, 30s) produced a robust EL-Ca^{2+} release of 37.69 ± 4.36 % (n= 15) of the total EL-Ca^{2+} luminal Ca^{2+}content, as reported by ELGA1 at the steady-state (***Figure 4E and J***). Upon application, ML-SA1 exhibited a lag time of ~20 s and it continued releasing Ca^{2+} once the agonist was washed out. Consecutive applications of ML-SA1 evoked responses of similar amplitude, indicating no desensitization of the channel. The time to refill the store after the washing out was ~5 min. Full concentration-effect relationship for the Ca^{2+} release response showed an EC_{50} value of 6.77 ± 0.9 μM (***Figures 4F* and *G***). Comparable responses were observed in TRPML1-expressing HeLa cells (***figure supplement 8)***. In accord, the response to ML-SA1 was selectively blocked by the specific TRPML-antagonist ML-SI1 **(*Figure* 4H *-figure supplement 8B*)** and expression of TRPML1 did not affect the response to IP_3 (***figure supplement 8C*).**

We also activated TRPML1 with its endogenous activator $PI(3,5)P_2$. As shown in ***Figure 4I***, $PI(3,5)P_2$ evoked EL-Ca^{2+} release in cells expressing TRPML1 albeit modestly compared to ML-SA1. Statistical quantification is summarized in ***Figure 4J***. The EL-Ca^{2+} release provoked by $PI(3,5)P_2$ was concentration-dependent (***Figure 4K and L).***

These data show that ELGA accurately reports the properties of a bona fide EL Ca^{2+} channel.

Finally, we used super-resolution microscopy to more accurately localise ELGA. As shown in ***Figure 4M -figure supplement 9 and supplement Table 2***, ELGA was resolved as clear puncta. There was little co-localization with an ER marker. However, we noted significant proximity between some ELGA-positive structures and ER, likely representing membrane contact sites between endo-lysosomes and the ER. In contrast, ELGA colocalised with TRPML1 at single EL vesicle ***(Figure 4M- figure supplement 9)***, consistent with our confocal analyses.

In sum, these data support the physical and functional targeting of ELGA to an EL compartment that is closely associated with but distinct from the ER.

Physiological IP_3-forming stimuli mobilize Ca^{2+} from endo-lysosomal Ca^{2+} stores

To further characterize the endo-lysosomal Ca^{2+} dynamics, we assessed luminal Ca^{2+} levels in intact cells. Addition of 1 mM $CaCl_2$ refilled the EL-Ca^{2+}store up to a steady-state of 234 ± 29 μM (n= 12) (***Figure 5A***).

To probe the functionality of IP3 receptors, we stimulated live cells with ATP which activates endogenous P2Y receptors or carbachol which activates muscarinic receptors. ATP and carbachol provoked fast and reversible EL-Ca^{2+}responses of 35.81 ± 2.34 % (n= 7) and 19.88 ± 1.87 % (n= 5), respectively (***Figure 5A and B***)***.*** ML-SA1 also produced reproducible responses in cells expressing TRPML1 although it was ineffective in wild type cells. Similar experiments were performed in polarised MDCK cells ***(Figure 5C).*** This cell type displayed a comparable steady-state EL-Ca^{2+} that was almost completely discharged upon cell activation with ATP (73.72 ± 16.85 %; n= 4).

Finally, we examined EL responses in a primary cell type. In mouse cortical astrocytes ***(Figure 5D)***, ML-SA1 application elicited a negligible effect in astrocytes whereas a subsequent pulse of ATP almost completely discharged the EL-Ca^{2+} store (87.68 ± 5.90 %; n= 6). A summary of the data is shown in ***Figure 5E***.

In sum, these data identify a widespread physiologically-relevant IP_3-sensitive Ca^{2+} store within the endo-lysosomal system.

DISCUSSION

Using a new genetically-encoded Ca^{2+} indicator based on aequorin, we demonstrate here the existence of a bona-fide endo-lysosomal Ca^{2+} store, able to accumulate a high [Ca^{2+}] and to release it upon physiological activation (***Figure 5F***).

Our results are best explained if this endo-lysosome is functionally coupled with the ER to accumulate Ca^{2+} via active transport such as via SERCA pumps. Although the two compartments work in parallel, they are distinct in the amount of Ca^{2+} that they can store, being significantly lower in the EL (~200-400 μM) than the ER (~400-500 μM) and in their sensitivity to expression of TRPML1, which selectively lowers the EL Ca^{2+} store. The EL-Ca^{2+} values are in agreement with previous reports (Narayanaswamy et al., 2019; Ronco et al., 2015) but contrast with others (Albrecht et al., 2015). The SERCA might be located at the EL membrane where it directly pumps Ca^{2+} into its lumen, or, alternatively, Ca^{2+} could be indirectly fuelled from the ER into the EL lumen, through an undetermined channel connecting the two organelles. The ER directly contacts the EL system through membrane contact sites (MCS), specially abundant in late endosomes, where they allow exchange of lipids and other molecules, including Ca^{2+} (Kilpatrick et al., 2013; Lee and Blackstone, 2020; Raiborg and Stenmark, 2015). Close association of ELGA-positive compartments with ER reported here might provide a route for uptake.

We show that activation of TRPML1 with ML-SA1/$PI(3,5P)_2$ and TPCs with NAADP produces luminal responses, but the latter were not consistent. Recent studies have shown that NAADP binds to soluble binding proteins to activate TPCs (Gunaratne et al., 2021; Roggenkamp et al., 2021; Zhang et al., 2021). It is possible that loss of these proteins upon permeabilization may account for NAADP insensitivity. Surprisingly, IP_3 consistently produced robust responses comparable to those evoked by bonafide EL channels. Functional IP_3 receptors have been documented in other acidic organelles such as secretory granules in professional secretory cell types (Gerasimenko et al., 2006; Santodomingo et al., 2008) and the acidocalcisome in Trypanosomes (Huang et al., 2013). But we are not aware of their presence within the EL system, which extends IP_3 action to potentially all cell types.

Our intact cell studies provide evidence that IP_3-sensitive stores can be tapped during physiological stimulation with IP_3-forming stimuli. The fast exit of Ca^{2+} from

the EL into the cytosol through IP_3 receptors would generate local cytosolic Ca^{2+} signals. These, in turn, could be amplified either via Ca^{2+}-induced Ca^{2+} release (CICR) through IP_3Rs (or RyRs in other cell types) present in the ER membrane to generate global signals. Indeed, IP_3Rs have been shown to be preferentially associate with the lysosomes at contact sites (Atakpa et al., 2019). Such coupling would be analogous to that triggering of Ca^{2+} signals by TRPML (Kilpatrick et al., 2016) or TPCs (Xu and Ren, 2015; Zhu et al., 2010). Our results are in line with the *chatter hypothesis* between the two organelles (Patel et al., 2010) and the essential role of the ER in the EL signal in various cell types (Garrity et al., 2016; López-Sanjurjo et al., 2013; Morgan et al., 2013; Yang et al., 2019) . Alternatively, local IP_3R-dependent Ca^{2+} signals may regulate endo-lysosomal function at basal (unstimulated) levels of IP3, again in analogy with TPCs and TRPML, which are well established in regulating membrane traffic (Pryor et al., 2000; Ruas et al., 2010).

In conclusion, our direct luminal Ca^{2+} measurements help to fill the gaps in our knowledge on the calcium signalling toolkit of the endo-lysosome system and provide new insight into the dynamics of these small acidic Ca^{2+} stores and their functional relationship with the ER Ca^{2+} stores.

FIGURE LEGENDS

Figure 1. Design, characterization and calibration of endo-lysosomal Ca^{2+} indicators. (A*)* Domain structure and mutations of the endo-lysosomal indicators drawn approximately at scale. VAMP7, vesicle-associated membrane protein 7; AEQ, aequorin; ELGA, endo-lysosomal GFP-Aequorin; ELGA1, endo-lysosomal GAP1. **(B)** Predicted topology of ELGA and ELGA1 Ca^{2+} probes within the endo-lysosome. **(C)** Representative confocal fluorescent images of equatorial plane of fixed MDCK cells transiently transfected with ELGA or ELGA1. Scale bar for both images, 10 µm. **(D)** ***Upper row:*** ELGA expressing HEK293T cells (*Left*, green) were immunostained with a specific anti-LAMP2 antibody (*Center*, magenta). Green and magenta images are merged (*Right, merge*). ***Lower row:*** Colocalization of ELGA (green) expressing HEK293T cells with the following organellar markers (magenta): ER, er-Ruby-GCaMP250 (ER); early endosome, immunostained with the anti-early endosome antigen 1 (EE); mitochondria (mt), immunostained with anti-TOM20 antibody. Scale bar for all images, 5 µm. **(E)** Effect of acidic pH on GA luminescence emission. *E.coli* recombinant GA apoprotein was reconstituted with native (*left*) or *n* (*right*) coelenterazine (CTZ) for 20 min at the indicated pH, and then subjected to luminescence emission assay triggered with 10 mM $CaCl_2$ (arrow) and measured at the same pH. Buffers used were: acetate for range 4.5-5.5 pH; Na-MOPS for 6 and 6.5 pH; and Na-Hepes for 7.2 pH. Each trace is the value normalized with respect to its background emission before addition of calcium. Each trace is the average of 3-4 independent experiments. **(F)** Luminescence activity of GA1 after regeneration with *n* coelenterazine at 7.2 or 4.5 pH. Peak value (mean ± S.E.M; n=3) obtained from an experiment similar to (E) performed at pHs 7.2 *(blue bar)* and 4.5 *(black bar)* or reconstituted with coelenterazine at pH 7.2 and switched to pH 4.5 to measure luminescence (*pink bar*). **(G)** Expression of ELGA in live HeLa and HEK293T cells. Scale bar, 10 µm. **(H)** Ca^{2+} titration curves of GA1 at pH 6.0 and 7.2. Each value is the mean ± S.E.M of 3-6 measurements obtained from two independent protein preparations.

Figure 2. Endo-lysosomal Ca^{2+} store accumulates Ca^{2+} via SERCA. (A) Representative EL-Ca^{2+} signals recorded in HEK293T cells transiently transfected with ELGA1. After Ca^{2+} depletion prior to reconstitution with coelenterazine *n*, cells were permeabilized in Ca^{2+}-free intracellular medium (containing 1 mM ATP) and

then perfused with 200 nM free [Ca^{2+}], as indicated. **(B)** Summary data (mean ± S.E.M.) of $[Ca^{2+}]_{EL}$ at steady-state obtained in populations of HEK293T, HeLa and MDCK cells with the number of independent transfections in parenthesis. **(C)** Cells were perfused as in (A) with an intracellular medium without ATP (-ATP) and reintroduced (1 mM) when indicated. **(D)** Cells were incubated with thapsigargin (1 μM) during the final 10 min of reconstitution followed by the application of the identical protocol described in (A). **(E)** Cells were perfused in an intracellular medium containing 2,5-di-tert-butylhydroquinone (tBHQ, 10 μM) followed by washout of the inhibitor. **(F)** Summary results (mean ± S.E.M.) with statistical analysis. ANOVA with Tukey's post hoc test was applied. **(G)** Cells were perfused as in (A) and, once the $[Ca^{2+}]_{EL}$ steady-state was reached, different conditions were tested (arrow): none (200 nM Ca^{2+}; Control), EGTA (0.1 mM)**,** tBHQ (10 μM), EGTA+ tBHQ, or removal of ATP (-ATP)**. (H)** Summary results of EL-Ca^{2+} exit responses shown in (G), obtained from at least 3 independent days. ANOVA with Tukey's post hoc test was applied. $p < 0.05$, ***$p < 0.001$, and ****$p < 0.0001$.

Figure 3. IP3 releases Ca^{2+} from the EL-Ca^{2+} store. (A) Representative response to IP_3 (2 μM, 30 s) in wt HEK293T cells expressing ELGA1. **(B)** Representative EL-Ca^{2+} release (in L/Lt ratio) upon application of four consecutive pulses (30s) of increasing concentrations of IP_3 (in μM). **(C)** Concentration-dependent response of EL-Ca^{2+} release (expressed as % of maximal response obtained with 30 μM IP_3) upon addition of increasing concentrations of IP_3 (0.01, 0.1, 1 and 10 μM). Each point is the mean ± S.E.M. of 3-4 values obtained from independent transfections. **(D)** Representative response to IP_3 (2 μM, 30 s) in IP_3R-null HEK293 (HEK-3KO) cell line expressing ELGA1. **(E)** Representative response to IP_3 in HEK-3KO cells transiently expressing IP3R1. **(F)** Statistical quantification of IP_3 induced-EL-Ca^{2+} release (mean ± S.E.M.) with the number of independent transfections in parenthesis. ANOVA with Tukey's post hoc test was applied. **(G)** Inhibition of the IP_3 EL-Ca^{2+} release by heparin (100 μg/mL) in ELGA1 expressing HEK293T cells. **(H)** Statistical quantification of heparin inhibition of IP_3 response. Data are expressed as mean ± S.E.M. In all bar graphs, numbers in parenthesis correspond to the number of independent transfections from at least 2-3 experiments. A Student´s t test was applied. ****$p < 0.0001$.

Figure 4. ELGA is located to the endo-lysosome, distinct to the ER. (A) Colocalization of ELGA fluorescence (green) with TRPML1-cherry (magenta) in either fixed or live HEK293T cells expressing both proteins. Scale bar in all images, 10 µm. **(B)** Quantitative colocalization analysis of confocal fluorescence microscopy images were expressed as Pearson's (*P*) correlation coefficient shown in (A). Each point represents an individual cell from at least 2 independent experiments (mean ± S.E.M). A Student's *t* test was applied. **(C)** Effect of expression of TRPML1 on the [Ca^{2+}] at steady-state recorded from HEK293T expressing either ELGA1 (EL) or ERGA1 (ER). Data are expressed as mean ± S.E.M. In all bar graphs, numbers in parenthesis correspond to the independent transfections. A Student's *t* test was applied. **(D)** Lack of correlation between resting [Ca^{2+}] in the ER and the EL recorded with ERGA1 or ELGA1, respectively, in six cell types: HEK293T (blue), TRPML1-expressing HEK293T (brown), IP3R-KO HEK (pink), HeLa (green), CHO (black) cells and cultured murine cortical astrocytes (orange). Data are expressed as mean ± S.E.M. ER-Ca^{2+} in astrocytes data are taken from (Rodríguez-Prados et al., 2020). **(E)** Representative ML-SA1 (20 µM, 30 s) responses inducing EL-Ca^{2+} releases (expressed as L/Lt) from HEK293T cells expressing TRPML1 measured with ELGA1. **(F)** Representative Ca^{2+} responses (expressed as L/Lt) to application of four consecutive pulses (30s) of increasing concentrations of ML-SA1. **(G)** Concentration-dependent EL-Ca^{2+} release (expressed as % of the maximal response) in response to increasing concentrations of ML-SA1. Each point is the mean ± S.E.M. of 3-4 values obtained from 3 independent experiments. **(H)** Effect of the TRPML1 inhibitor MLSI-1 (10 µM) on the ML-SA1 (20 µM) response (expressed as L/Lt) in TRPML1 transfected HEK293T cells. **(I)** Effect of PI(3,5)P_2 (1 µM) on the EL-Ca^{2+} release in TRPML1 expressing HEK293T cells. **(J)** Summary results and statistical quantification of EL-Ca^{2+} release responses under various experimental conditions. Control non-transfected or TRPML1 transfected HEK293T cells. Percentage of response related to total $[Ca^{2+}]_{EL}$ at the steady-state is indicated. Data are expressed as mean ± S.E.M. and numbers in parenthesis indicate total n of experiments. A Tukey's post hoc test (MLSA1 data) and a Student's *t* test (PI(3,5)P_2) were applied. **(K)** Concentration-dependent response (expressed as L/Lt) for EL-Ca^{2+} release upon increasing concentrations of PI(3,5)P_2. **(L)** Summary results and statistical significance of the responses determined from three experiments like that shown in (K)**.** Results are expressed as mean ± S.E.M.

An ANOVA with a Tukey's post hoc test was applied. **(M)** Super-resolution images of localization of ELGA to the EL system. Scale bar for both images, 5 µm. **Left**, HEK293T cells expressing ELGA (*green*) together with an ER marker (*magenta*). All images are maximal Z projections. Arrows indicate putative membrane contact sites between endo-lysosome and the ER. **Right**, HEK293T cells expressing ELGA (*green*) and TRPML1 (*magenta*). Maximal Z projections. *$p < 0.05$, **$p < 0.01$, ***$p < 0.001$, and ****$p < 0.0001$.

Figure 5. Physiological endo-lysosomal Ca^{2+} release. (A) Representative EL-Ca^{2+} responses (in L/Lt) to agonists (ML-SA1, 20 µM; ATP, 100 µM; Carbachol, (CCh),100 µM) in intact HEK293T cells expressing ELGA1. **(B)** Similar to (A), in transiently expressing TRPML1 HEK293T cells. **(C)** Protocol similar to (A) applied in MDCK cells. **(D)** Protocol similar to (A) applied in astrocytes. **(E)** Summary results of EL-Ca^{2+} release induced by ML-SA1 and ATP in different cell types or conditions. Data are expressed as mean ± S.E.M. and numbers in brackets correspond to the total number of experiments. Responses are in percentages related to total $[Ca^{2+}]_{EL}$ at the steady-state. **(F)** A proposed model of Ca^{2+} dynamics in the endo-lysosome (see text for explanation).

METHODS

Gene construction

H. sapiens VAMP7 cDNA was amplified by PCR using specific primers (#324; forward: 5'-CCAaagcttGCCACCATGGCGATTCTTTTT-3'; #325; reverse: 5'-ATaagcttTTTCTTCACACAGCTTGGCCATG-3'; *HindIII* sites are in lowercase). This fragment was digested with *HindIII* and inserted upstream of the *HindIII* fragment encoding the GA or the GA1 cDNAs, in the pHSV plasmid leading to pHSV-ELGA or pHSV-ELGA1 plasmids, respectively. The GA gene is a fusion of EGFP and aequorin (Manjarres et al., 2008) containing the D119A mutation (Kendall et al., 1992). The GA1 (previously described as GAP1) gene is a fusion of GFP (C3) and aequorin containing the mutations D117A, D119A and D163A (Rodriguez-Garcia et al., 2014). For expression in bacteria, GA or GA1 cDNAs were cloned into the pET28a vector. For measurements of ER-Ca^{2+}, the pHSV-ERGA1 (previously described as erGAP1) was used (Rodriguez-Prados et al., 2015).

Virus production

pHSV-ELGA or pHSV-ELGA1 were packaged into HSV-1 amplicon particles using a deletion mutant packaging system. Briefly, these plasmids were transfected into 2-2 cells and then, infected with a defective 5dl 1.2 helper virus. Titration was performed as previously described (Alonso et al., 1996; Lim et al., 1996).

Bacterial expression of GA and GA1 proteins

GA or GA1 cloned in pET28a were transformed in *E. coli* BL21 (Stratagene). Bacteria were grown at 37º C to A_{600} >0.6 in LB containing 40 mg/L kanamycin and induced with 0.05 mM isopropyl β-D-thiogalactoside (IPTG) for 5h at 30º. Cells were then pelleted by centrifugation at 6000 g for 30 min and sonicated in a buffer containing (in mM): NaCl, 50; DTT, 0.5; Tris-HCl 20, pH 7.5; and Roche protein inhibitors. The bacterial lysate was centrifuged at 30,000 g for 10 min. Protein was purified by using a HisPur Ni-NTA resin (ThermoFisher, 88222). Protein quantification was performed by Bradford (range 20-60 µg/µL).

Bioluminescence activity at various pHs

Measurements were performed in the Tecan Genios Pro 96-well plate reader. Recombinant *E.coli* GA or GA1 protein was reconstituted with coelenterazine *n* (1

μM) for 20 min and then 5-10 μL were aliquoted into each well to a final volume of 100 μL with a buffer containing (in mM): KCl, 140; $MgCl_2$, 1; MOPS/Tris, 20, pH 7.2. The effects of pH were monitored using different buffers for each pH range: acetate for pH in the range 4.5-5.5; MOPS/Na for pH range 6; and Hepes/Na for pH 7.2. Maximal luminescence was acquired by injecting 10-25 μL of saturating (50 mM) Ca^{2+}. Calibrations were performed in Ca^{2+}-free medium (0.1 mM EGTA added), or in the same solutions containing increasing Ca^{2+} concentrations between 50 μM and 50 mM. This calcium solution (10 μL) was injected with a first injector, read for 15 seconds and then a saturating calcium solution (10 mM) was injected with a second injector.

Cell culture and gene expression

HeLa (CCL-2), HEK 293-T (CLR-1573), CHO- K1 (CCL-61) or MDCK cells (CCL-34), were all purchased from ATCC. All cells were maintained in Dulbecco's Modified Eagle Medium (DMEM, Invitrogen) supplemented with 10% fetal bovine serum (FBS, Sigma) , 2 mM L-glutamine, 100 μg/ml streptomycin and 100 U/ml penicillin. IP3R-null HEK293 (HEK-3KO) cells (Alzayady et al., 2016) were maintained in DMEM/F-12 with GlutaMAX (ThermoFisher) supplemented with 10%, FBS. Periodic PCR screening confirmed that all cells were free of mycoplasma infection.

Mouse cortical astrocytes were isolated using the protocol described previously (Rodríguez-Prados et al., 2020) with the approval of the Institutional Animal Care and Use Committee at the University of Valladolid (ethics approval reference number: 10207729). Briefly, cortices were dissected from three P2-3 C57BL/6J Crl (Charles Rivers) mice in cold HBSS and digested with 0.5 mg/mL papain and 0.04 mg/mL DNase dissolved in a Ca^{2+}- and Mg-free HBSS with 10 mM glucose and 0.1% bovine serum albumin (BSA) at 37ºC for 20 min. Cells were resuspended with Minimal Essential Medium (MEM) supplemented with 2 mM glutamax, 27 mM glucose, 100 U/mL penicillin, 100 μg/mL streptomycin and 10% (v/v) horse serum, and plated on a poly-L-lysine coated 75 cm^2 flask. After 2 and 7 days, flasks were slapped to remove neurons and other loosely attached cells such as microglia and oligodendrocytes. After one week, cells were trypsinized and seeded in the same

medium onto poly-L-lysine coated 12 mm-diameter glass coverslips at a density of 2.5 x 10^4 cells/coverslip. The cultures were used within 1-2 weeks.

Cells were transiently transfected with 0. 2 µg (HEK293T) or 0.2-0.5 µg (HeLa) pHSV-ELGA or pHSV-ELGA1 using Lipofectamine 2000 (Invitrogen), according to the manufacturer's instructions. In some experiments, this plasmid was cotransfected with other plasmids encoding: EGFP-trpML1 (0.02 µg); mCherry-trpML1 (0.05 µg; Addgene #135189); er-Ruby-GCaMP210 (0.5 µg) (de Juan-Sanz et al., 2017); IP3R1 (0.02 µg). Stably transfected HeLa clones expressing ELGA were generated by cotransfection of pHSV-ELGA and pcDNA3 (carrying the *neomycin* gene). GFP positive cells were enriched by sorting in a FACSAria II followed by antibiotic selection with 800 µg/mL G418 and single cell cloning was performed by limited dilution. ELGA-HeLa clones (No. 3 and 6) were maintained with 100 µg/mL G418.

ELGAs expression in mouse cortical astrocyte cultures was achieved by infection with herpes HSV-ELGA, HSV-ELGA1 or HSV-ERGA1 (previously named erGAP1) amplicons at a multiplicity of infection (moi) ranging between 0.01 and 0.1, one day before use.

Ca^{2+} bioluminescence measurements

Cells expressing ELGA1 (or ELGA in some experiments) were seeded on 4-well plates at a density of 8 × 10^4 (HeLa, CHO, or MDCK cells) or 2 × 10^5 (HEK-293T and HEK-3KO cells). HEK cells were poly-L-lysine coated. Cells were Ca^{2+} depleted by incubation with the reversible sarco-endoplasmic reticulum Ca^{2+}-ATPase (SERCA) inhibitor 2,5-di-tert-butylhydroquinone (TBH; 10 µM) in the extracellular buffer (145 mM NaCl; 5 mM KCl; 1 mM MgCl2; 10 mM glucose; 10 mM Na-HEPES, pH 7.4) supplemented with 0.5 mM EGTA for 10 min at 22ºC. Apo-aequorin was then reconstituted by incubation with 1 µM *n* coelenterazine in the same medium during 1-2 hour prior to measurements. Cells were then placed in the luminometer (Cairn Research, UK). Light acquisition was recorded as cps each second.

Intact cells were perfused (5 mL/min) with the extracellular buffer containing 1 mM $CaCl_2$ plus additions as stated. In the experiments with permeabilized cells, perfusion was performed with an intracellular-like (IL) medium with the following composition (in mM): KCl, 140; KH_2PO4, 1; $MgCl_2$ 1; Mg-ATP, 1; sodium succinate,

2; sodium-pyruvate, 1; Na-HEPES, 20, pH 7.2. The cells were permeabilized by perfusion of digitonin (50 µM) in the IL medium containing 0.5 mM EGTA during 1 min. The digitonin was washed out and the cells were then switched to IL medium containing 200 nM Ca^{2+}made by blending titrated solutions of EGTA and EGTA-Ca^{2+} in the required amounts, calculated using the program MaxChelator (Patton et al., 2004). If not stated otherwise, all stimuli or drugs were dissolved and applied in the IL-buffer containing 200 nM Ca^{2+} during 30s, as indicated in the graphs. At the end of each run, cells were lysed with 100 µM digitonin in a 10 mM $CaCl_2$ solution to release all the remaining aequorin luminescence. The EL-Ca^{2+} was expressed as luminescence at a certain time point (L) divided by total luminescence till that moment (L/Lt). All measurements were performed at 22ºC. Calibration curve allowed to calculate L/Lt into [Ca^{2+}] (µM) (Rodriguez-Prados et al., 2015).

Immunofluorescence

2-5 x 10^4 HEK cells were seeded onto 12 mm-glass coverslips and fixed, either with cold 100% methanol or with 4% PFA in PBS for 20 min, followed by incubation with 10% goat serum, 0.2% saponin (or 1% goat serum with 0.1% Tween-20 in some experiments) in PBS for 20 min at 22 ºC. The incubation with the primary antibody was performed overnight at 4ºC. The following primary antibodies were used: mouse anti-LAMP2 (H4B4) antibody (1:100; DSHB / University of Iowa); mouse anti-EEA1 antibody (1:200; BD Transduction Laboratories); mouse anti-TOM20 (1:100; Santa Cruz). The secondary antibodies (anti-mouse Alexa Fluor 568-conjugated antibodies) were incubated for 1h at 22 ºC. Nuclei were stained with 4',6-diamidino-2-phenylindole (DAPI). Cells were mounted with VectashieldR (Vector).

Confocal microscopy

Intact or fixed cells were imaged under a 63 X Plan-Apochromat (NA 1.4) oil immersion objective using a confocal microscope (SP5 Leica) equipped with a white laser. Images were analyzed with ImageJ software using the JACoP plugin (Bolte and Cordelières, 2006). Super-resolution (1 µm) images were obtained with a SP8-STED Leica confocal microscope using a 100 X objective and the LAS-X deconvolution software.

Statistical analysis

Results are expressed as mean ± S.E.M., as indicated. Data were analyzed with the GraphPad Prism 9 software (San Diego, CA, USA). Statistical significance between two groups was analyzed by the unpaired Student t test, whereas more than two groups were compared using one-way analysis of variance (ANOVA) and Tukey post-test analysis. Differences were considered statistically significant when probability (*p*) values were less or equal than 0.05 (*), 0.01 (**), 0.001 (***) or 0.0001(****). Sample sizes (n) refer to independent cell wells from, at least, 3 different days. Individual traces show representative experiments.

Funding

This work was supported by grants PID2020-116086RB-I00 from the Ministerio de Ciencia e Innovación de España and by the Programa Estratégico del Instituto de Biología y Genética Molecular (IBGM), Escalera de Excelencia, Junta de Castilla y León (Ref. CLU-2019-02), and the BBSRC, UK (BB/T015853/1 and BB/W01551X/1).

Credit authorship contribution statement

FJA made the original observations; BC, PT-V, AD-L, CR, FJA and JR-R performed investigation, formal analysis, and interpretation of data; JG-S, SP and MTA provided conceptualization and funding acquisition; MTA wrote original draft; all authors reviewed and edited the manuscript.

Declaration of Competing interest

The authors declare no competing financial interests.

Acknowledgments

We thank Dr. H. Xu for the VAMP7 plasmid; Dr. De Juan-Sanz for erRuby-GCaMP210; Dr. D.Yule for HEK-3KO cells; and, C. Taylor for IP_3R1 cDNA. We also thank Dr. M. Montero, J. Alvarez and T. Schimmang for their valuable comments and suggestions. We also thank I. López and J. Fernández, as well as the Servicio de Microscopía, (C.I.C., Salamanca), for technical assistance.

REFERENCES

Albrecht, T., Zhao, Y., Nguyen, T. H., Campbell, R. E. and Johnson, J. D. (2015). Fluorescent biosensors illuminate calcium levels within defined beta-cell endosome subpopulations. *Cell calcium* **57**, 263-274.

Alonso, M. T., Lim, F., Nunez, L., Represa, J., Giraldez, F. and Schimmang, T. (1996). HSV-1 vector mediated transfer of BDNF into cerebellar granule cells. *Neuroreport* **7**, 3105-3108.

Alzayady, K. J., Wang, L., Chandrasekhar, R., Wagner, L. E., 2nd, Van Petegem, F. and Yule, D. I. (2016). Defining the stoichiometry of inositol 1,4,5-trisphosphate binding required to initiate Ca2+ release. *Science signaling* **9**, ra35.

Atakpa, P., van Marrewijk, L. M., Apta-Smith, M., Chakraborty, S. and Taylor, C. W. (2019). GPN does not release lysosomal Ca(2+) but evokes Ca(2+) release from the ER by increasing the cytosolic pH independently of cathepsin C. *J Cell Sci* **132**.

Bolte, S. and Cordelières, F. P. (2006). A guided tour into subcellular colocalization analysis in light microscopy. *J Microsc* **224**, 213-232.

Christensen, K. A., Myers, J. T. and Swanson, J. A. (2002). pH-dependent regulation of lysosomal calcium in macrophages. *J Cell Sci* **115**, 599-607.

de Juan-Sanz, J., Holt, G. T., Schreiter, E. R., de Juan, F., Kim, D. S. and Ryan, T. A. (2017). Axonal Endoplasmic Reticulum Ca(2+) Content Controls Release Probability in CNS Nerve Terminals. *Neuron* **93**, 867-881.e866.

Dong, X. P., Shen, D., Wang, X., Dawson, T., Li, X., Zhang, Q., Cheng, X., Zhang, Y., Weisman, L. S., Delling, M., et al. (2010). PI(3,5)P(2) controls membrane trafficking by direct activation of mucolipin Ca(2+) release channels in the endolysosome. *Nature communications* **1**, 38.

Garrity, A. G., Wang, W., Collier, C. M., Levey, S. A., Gao, Q. and Xu, H. (2016). The endoplasmic reticulum, not the pH gradient, drives calcium refilling of lysosomes. *eLife* **5**.

Geller, A. I. (1991). A system, using neural cell lines, to characterize HSV-1 vectors containing genes which affect neuronal physiology, or neuronal promoters. *J Neurosci Methods* **36**, 91-103.

Gerasimenko, J. V., Sherwood, M., Tepikin, A. V., Petersen, O. H. and Gerasimenko, O. V. (2006). NAADP, cADPR and IP3 all release Ca2+ from the endoplasmic reticulum and an acidic store in the secretory granule area. *J Cell Sci* **119**, 226-238.

Gunaratne, G. S., Brailoiu, E., He, S., Unterwald, E. M., Patel, S., Slama, J. T., Walseth, T. F. and Marchant, J. S. (2021). Essential requirement for JPT2 in NAADP-evoked Ca²⁺ signaling. *Science signaling* **14**, eabd5605.

Huang, G., Bartlett, P. J., Thomas, A. P., Moreno, S. N. and Docampo, R. (2013). Acidocalcisomes of Trypanosoma brucei have an inositol 1,4,5-trisphosphate

receptor that is required for growth and infectivity. *Proc Natl Acad Sci U S A* **110**, 1887-1892.

Johnson, F. H. and Shimomura, O. (1978). [30] Introduction to the bioluminescence of medusae, with special reference to the photoprotein aequorin. In *Methods in Enzymology*, pp. 271-291: Academic Press.

Kendall, J. M., Sala-Newby, G., Ghalaut, V., Dormer, R. L. and Campbell, A. K. (1992). Engineering the CA(2+)-activated photoprotein aequorin with reduced affinity for calcium. *Biochem Biophys Res Commun* **187**, 1091-1097.

Kilpatrick, B. S., Eden, E. R., Schapira, A. H., Futter, C. E. and Patel, S. (2013). Direct mobilisation of lysosomal Ca2+ triggers complex Ca2+ signals. *J Cell Sci* **126**, 60-66.

Kilpatrick, B. S., Yates, E., Grimm, C., Schapira, A. H. and Patel, S. (2016). Endo-lysosomal TRP mucolipin-1 channels trigger global ER Ca2+ release and Ca2+ influx. *Journal of Cell Science* **129**, 3859-3867.

Lee, C. A. and Blackstone, C. (2020). ER morphology and endo-lysosomal crosstalk: Functions and disease implications. *Biochim Biophys Acta Mol Cell Biol Lipids* **1865**, 158544.

Lim, F., Hartley, D., Starr, P., Lang, P., Song, S., Yu, L., Wang, Y. and Geller, A. I. (1996). Generation of high-titer defective HSV-1 vectors using an IE 2 deletion mutant and quantitative study of expression in cultured cortical cells. *Biotechniques* **20**, 460-469.

Lloyd-Evans, E., Morgan, A. J., He, X., Smith, D. A., Elliot-Smith, E., Sillence, D. J., Churchill, G. C., Schuchman, E. H., Galione, A. and Platt, F. M. (2008). Niemann-Pick disease type C1 is a sphingosine storage disease that causes deregulation of lysosomal calcium. *Nature medicine* **14**, 1247-1255.

López-Sanjurjo, C. I., Tovey, S. C., Prole, D. L. and Taylor, C. W. (2013). Lysosomes shape Ins(1,4,5)P3-evoked Ca2+ signals by selectively sequestering Ca2+ released from the endoplasmic reticulum. *J Cell Sci* **126**, 289-300.

Manjarres, I. M., Chamero, P., Domingo, B., Molina, F., Llopis, J., Alonso, M. T. and Garcia-Sancho, J. (2008). Red and green aequorins for simultaneous monitoring of Ca2+ signals from two different organelles. *Pflugers Arch* **455**, 961-970.

Melchionda, M., Pittman, J. K., Mayor, R. and Patel, S. (2016). Ca2+/H+ exchange by acidic organelles regulates cell migration in vivo. *J Cell Biol* **212**, 803-813.

Mindell, J. A. (2012). Lysosomal acidification mechanisms. *Annual review of physiology* **74**, 69-86.

Mitchell, K. J., Pinton, P., Varadi, A., Tacchetti, C., Ainscow, E. K., Pozzan, T., Rizzuto, R. and Rutter, G. A. (2001). Dense core secretory vesicles revealed as a dynamic Ca(2+) store in neuroendocrine cells with a vesicle-associated membrane protein aequorin chimaera. *J Cell Biol* **155**, 41-51.

Morgan, A. J., Davis, L. C., Wagner, S. K., Lewis, A. M., Parrington, J., Churchill, G. C. and Galione, A. (2013). Bidirectional Ca^{2+} signaling occurs between the endoplasmic reticulum and acidic organelles. *J Cell Biol* **200**, 789-805.

Morgan, A. J., Platt, F. M., Lloyd-Evans, E. and Galione, A. (2011). Molecular mechanisms of endolysosomal Ca2+ signalling in health and disease. *The Biochemical journal* **439**, 349-374.

Narayanaswamy, N., Chakraborty, K., Saminathan, A., Zeichner, E., Leung, K., Devany, J. and Krishnan, Y. (2019). A pH-correctable, DNA-based fluorescent reporter for organellar calcium. *Nature methods* **16**, 95-102.

Patel, S. and Docampo, R. (2010). Acidic calcium stores open for business: expanding the potential for intracellular Ca2+ signaling. *Trends in cell biology* **20**, 277-286.

Patel, S., Marchant, J. S. and Brailoiu, E. (2010). Two-pore channels: Regulation by NAADP and customized roles in triggering calcium signals. *Cell calcium* **47**, 480-490.

Patton, C., Thompson, S. and Epel, D. (2004). Some precautions in using chelators to buffer metals in biological solutions. *Cell calcium* **35**, 427-431.

Pryor, P. R., Mullock, B. M., Bright, N. A., Gray, S. R. and Luzio, J. P. (2000). The role of intraorganellar Ca(2+) in late endosome-lysosome heterotypic fusion and in the reformation of lysosomes from hybrid organelles. *J Cell Biol* **149**, 1053-1062.

Pryor, P. R., Mullock, B. M., Bright, N. A., Lindsay, M. R., Gray, S. R., Richardson, S. C., Stewart, A., James, D. E., Piper, R. C. and Luzio, J. P. (2004). Combinatorial SNARE complexes with VAMP7 or VAMP8 define different late endocytic fusion events. *EMBO reports* **5**, 590-595.

Raiborg, C. and Stenmark, H. (2015). An ER clamp for endosome fission. *Embo j* **34**, 136-137.

Rodriguez-Garcia, A., Rojo-Ruiz, J., Navas-Navarro, P., Aulestia, F. J., Gallego-Sandin, S., Garcia-Sancho, J. and Alonso, M. T. (2014). GAP, an aequorin-based fluorescent indicator for imaging Ca2+ in organelles. *Proc Natl Acad Sci U S A* **111**, 2584-2589.

Rodriguez-Prados, M., Rojo-Ruiz, J., Aulestia, F. J., Garcia-Sancho, J. and Alonso, M. T. (2015). A new low-Ca(2)(+) affinity GAP indicator to monitor high Ca(2)(+) in organelles by luminescence. *Cell calcium* **58**, 558-564.

Rodríguez-Prados, M., Rojo-Ruiz, J., García-Sancho, J. and Alonso, M. T. (2020). Direct monitoring of ER Ca(2+) dynamics reveals that Ca(2+) entry induces ER-Ca(2+) release in astrocytes. *Pflugers Archiv : European journal of physiology* **472**, 439-448.

Roggenkamp, H. G., Khansahib, I., Hernandez, C. L., Zhang, Y., Lodygin, D., Krüger, A., Gu, F., Möckl, F., Löhndorf, A., Wolters, V., et al. (2021). HN1L/JPT2: A signaling protein that connects NAADP generation to Ca(2+) microdomain formation. *Science signaling* **14**.

Ronco, V., Potenza, D. M., Denti, F., Vullo, S., Gagliano, G., Tognolina, M., Guerra, G., Pinton, P., Genazzani, A. A., Mapelli, L., et al. (2015). A novel Ca^{2+}-mediated cross-talk between endoplasmic reticulum and acidic organelles: implications for NAADP-dependent Ca^{2+} signalling. *Cell calcium* **57**, 89-100.

Ruas, M., Rietdorf, K., Arredouani, A., Davis, L. C., Lloyd-Evans, E., Koegel, H., Funnell, T. M., Morgan, A. J., Ward, J. A., Watanabe, K., et al. (2010). Purified TPC isoforms form NAADP receptors with distinct roles for Ca(2+) signaling and endolysosomal trafficking. *Curr Biol* **20**, 703-709.

SantoDomingo, J., Fonteriz, R. I., Lobaton, C. D., Montero, M., Moreno, A. and Alvarez, J. (2010). Ca2+ dynamics in the secretory vesicles of neurosecretory PC12 and INS1 cells. *Cell Mol Neurobiol* **30**, 1267-1274.

Santodomingo, J., Vay, L., Camacho, M., Hernández-Sanmiguel, E., Fonteriz, R. I., Lobatón, C. D., Montero, M., Moreno, A. and Alvarez, J. (2008). Calcium dynamics in bovine adrenal medulla chromaffin cell secretory granules. *The European journal of neuroscience* **28**, 1265-1274.

Shen, D., Wang, X., Li, X., Zhang, X., Yao, Z., Dibble, S., Dong, X. P., Yu, T., Lieberman, A. P., Showalter, H. D., et al. (2012). Lipid storage disorders block lysosomal trafficking by inhibiting a TRP channel and lysosomal calcium release. *Nature communications* **3**, 731.

Shimomura, O., Johnson, F. H. and Morise, H. (1974). Mechanism of the luminescent intramolecular reaction of aequorin. *Biochemistry* **13**, 3278-3286.

Vats, S. and Galli, T. (2022). Role of SNAREs in Unconventional Secretion-Focus on the VAMP7-Dependent Secretion. *Frontiers in cell and developmental biology* **10**, 884020.

Xu, H. and Ren, D. (2015). Lysosomal physiology. *Annual review of physiology* **77**, 57-80.

Yang, J., Zhao, Z., Gu, M., Feng, X. and Xu, H. (2019). Release and uptake mechanisms of vesicular Ca(2+) stores. *Protein & cell* **10**, 8-19.

Zhang, J., Guan, X., Shah, K. and Yan, J. (2021). Lsm12 is an NAADP receptor and a two-pore channel regulatory protein required for calcium mobilization from acidic organelles. *Nature communications* **12**, 4739.

Zhu, M. X., Ma, J., Parrington, J., Calcraft, P. J., Galione, A. and Evans, A. M. (2010). Calcium signaling via two-pore channels: local or global, that is the question. *American journal of physiology. Cell physiology* **298**, C430-441.

Fig.1

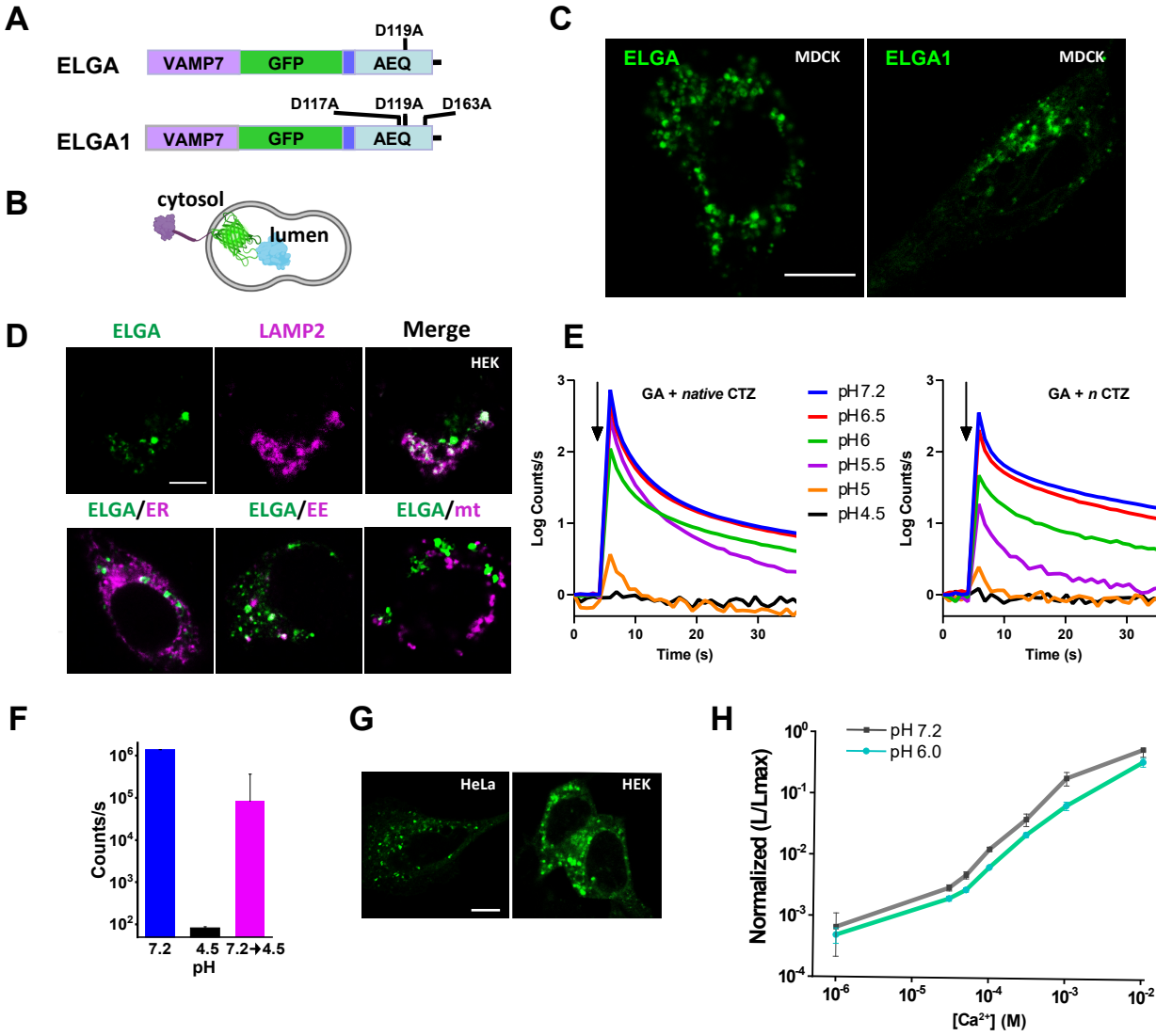
A
ELGA
VAMP7
GFP
AEQ
D119A
ELGA1
D117A
D119A
D163A
B
cytosol
lumen
C
ELGA
MDCK
ELGA1
MDCK
D
ELGA
LAMP2
Merge
HEK
ELGA/ER
ELGA/EE
ELGA/mt
E
GA + native CTZ
GA + n CTZ
pH7.2
pH6.5
pH6
pH5.5
pH5
pH4.5
Log Counts/s
Time (s)
F
Counts/s
7.2
4.5
7.2→4.5
pH
G
HeLa
HEK
H
pH 7.2
pH 6.0
Normalized (L/Lmax)
[Ca2+] (M)

Fig.2

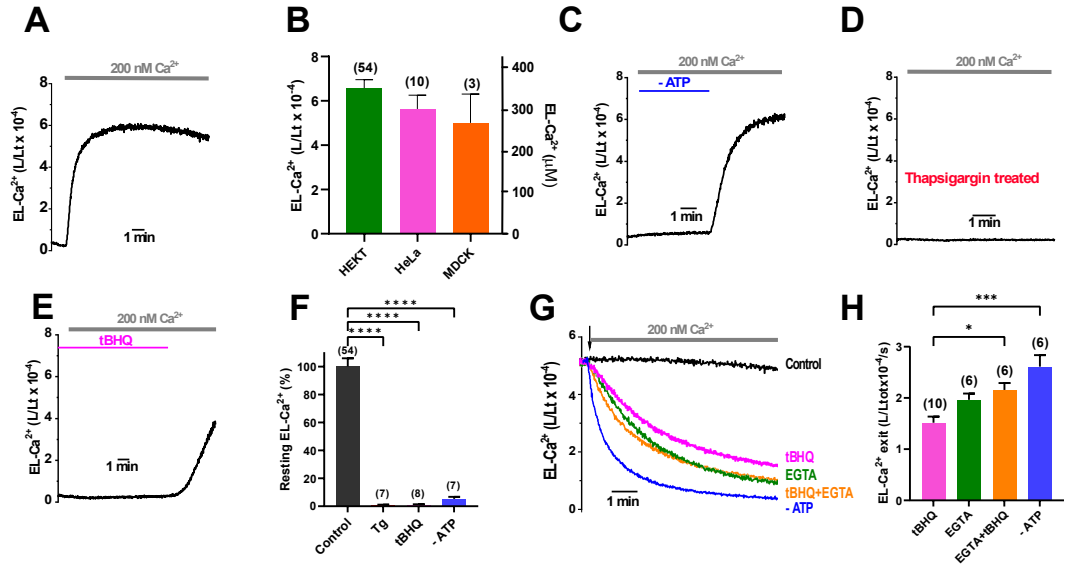
A
200 nM Ca2+
EL-Ca2+ (L/Lt x 10-4)
1 min
B
(54)
(10)
(3)
EL-Ca2+ (L/Lt x 10-4)
EL-Ca2+ (μM)
HEKT
HeLa
MDCK
C
200 nM Ca2+
- ATP
EL-Ca2+ (L/Lt x 10-4)
1 min
D
200 nM Ca2+
Thapsigargin treated
EL-Ca2+ (L/Lt x 10-4)
1 min
E
200 nM Ca2+
tBHQ
EL-Ca2+ (L/Lt x 10-4)
1 min
F
****
****
****
(54)
(7)
(8)
(7)
Resting EL-Ca2+ (%)
Control
Tg
tBHQ
- ATP
G
200 nM Ca2+
Control
tBHQ
EGTA
tBHQ+EGTA
- ATP
EL-Ca2+ (L/Lt x 10-4)
1 min
H
***
*
(10)
(6)
(6)
(6)
EL-Ca2+ exit (L/Lt.tx10-4/s)
tBHQ
EGTA
EGTA+tBHQ
- ATP

Fig. 3

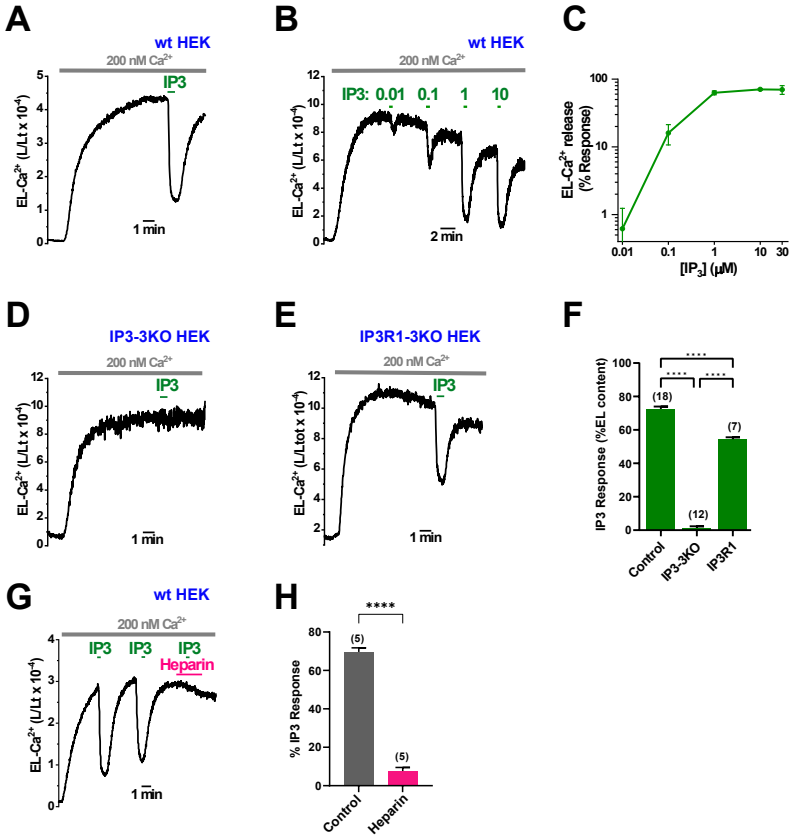
A
wt HEK
200 nM Ca2+
IP3
EL-Ca2+ (L/Lt x 10-4)
1 min
B
wt HEK
200 nM Ca2+
IP3: 0.01 0.1 1 10
EL-Ca2+ (L/Lt x 10-4)
2 min
C
EL-Ca2+ release (% Response)
[IP3] (μM)
D
IP3-3KO HEK
200 nM Ca2+
IP3
EL-Ca2+ (L/Lt x 10-4)
1 min
E
IP3R1-3KO HEK
200 nM Ca2+
IP3
EL-Ca2+ (L/Ltot x 10-4)
1 min
F
IP3 Response (%EL content)
(18)
(12)
(7)
Control
IP3-3KO
IP3R1
G
wt HEK
200 nM Ca2+
IP3 IP3 IP3
Heparin
EL-Ca2+ (L/Lt x 10-4)
1 min
H
% IP3 Response
(5)
(5)
Control
Heparin

Fig. 4

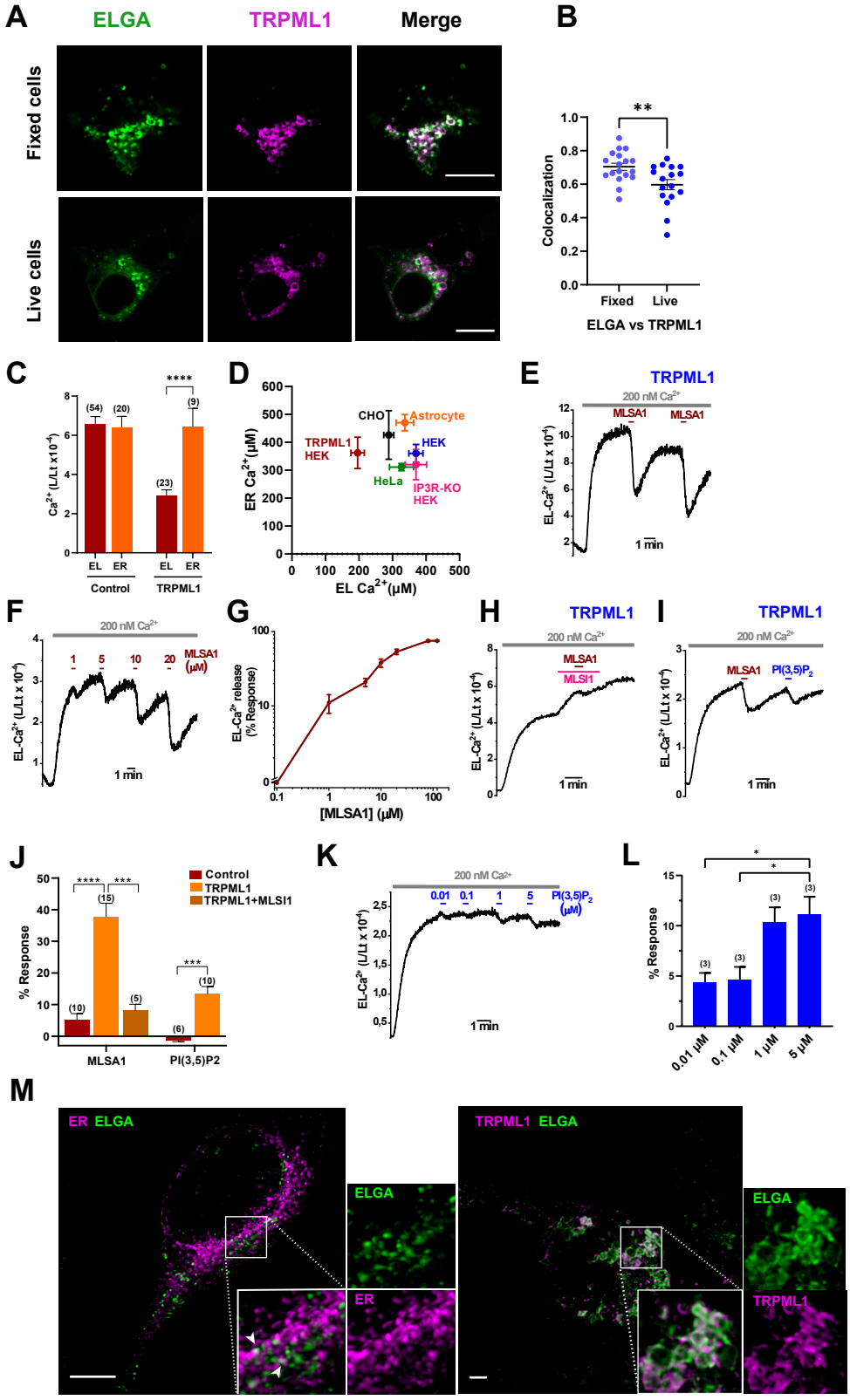
A
ELGA
TRPML1
Merge
Fixed cells
Live cells
B
Colocalization
Fixed
Live
ELGA vs TRPML1
C
Control
TRPML1
D
CHO
Astrocyte
TRPML1 HEK
HEK
HeLa
IP3R-KO HEK
ER Ca2+ (µM)
EL Ca2+ (µM)
E
TRPML1
200 nM Ca2+
MLSA1
1 min
F
MLSA1 (µM)
G
EL-Ca2+ release (% Response)
[MLSA1] (µM)
H
MLSI1
I
PI(3,5)P2
J
Control
TRPML1
TRPML1+MLSI1
% Response
MLSA1
PI(3,5)P2
K
PI(3,5)P2 (µM)
L
0.01 µM
0.1 µM
1 µM
5 µM
M
ER ELGA
ELGA
ER
TRPML1 ELGA
ELGA
TRPML1

Fig.5

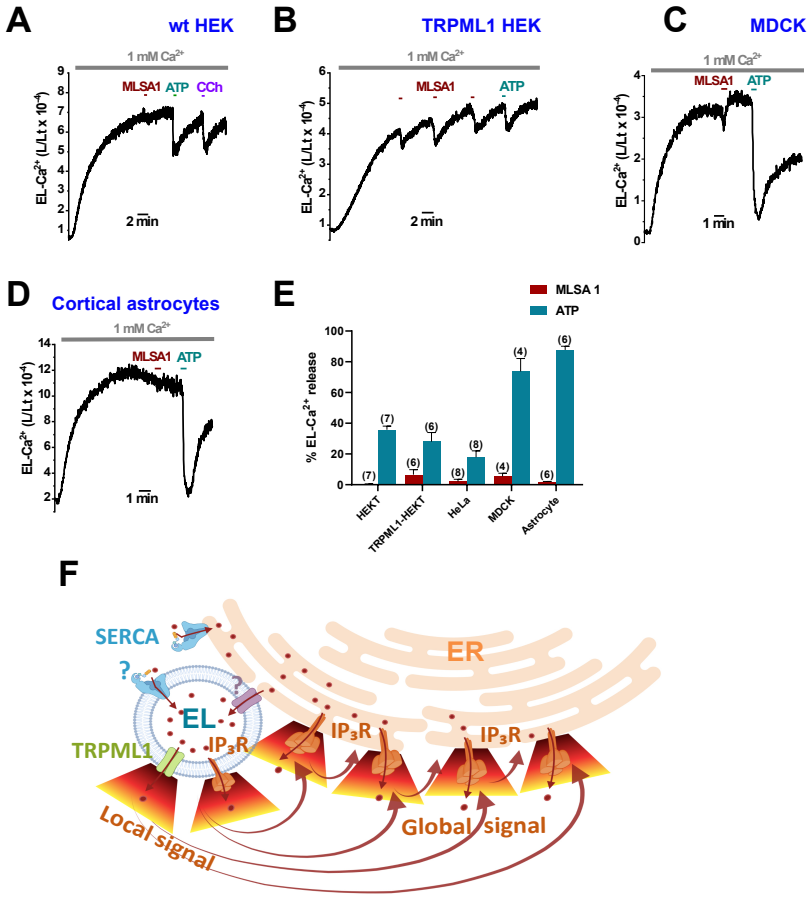
A
wt HEK
1 mM Ca2+
MLSA1
ATP
CCh
EL-Ca2+ (L/Lt x 10-4)
2 min
B
TRPML1 HEK
1 mM Ca2+
MLSA1
ATP
EL-Ca2+ (L/Lt x 10-4)
2 min
C
MDCK
1 mM Ca2+
MLSA1
ATP
EL-Ca2+ (L/Lt x 10-4)
1 min
D
Cortical astrocytes
1 mM Ca2+
MLSA1
ATP
EL-Ca2+ (L/Lt x 10-4)
1 min
E
MLSA 1
ATP
% EL-Ca2+ release
HEKT
TRPML1-HEKT
HeLa
MDCK
Astrocyte
F
SERCA
?
ER
EL
TRPML1
IP3R
IP3R
IP3R
Local signal
Global signal

Direct measurements of luminal Ca^{2+} with endo-lysosomal GFP-aequorin (ELGA) reveal functional IP_3 receptors

Calvo B[1*], Torres-Vidal P[1*], Delrio-Lorenzo A[2], Rodriguez C[1], Aulestia FJ[3], Rojo-Ruiz J[1], Garcia-Sancho J[1], Patel S[4**] and Alonso MT[1**]

Supplemental material:

Figure supplement 1. GA and GA1 bioluminescent Ca^{2+} sensors.

Figure supplement 2. Effect of acidic pH on aequorin luminescence emission.

Figure supplement 3. EL-Ca^{2+} dynamics in various cell types.

Figure supplement 4. Effects of Bafilomycin A1 on the EL-Ca^{2+} dynamics.

Figure supplement 5. NAADP evoked Ca^{2+} release from the endo-lysosome.

Figure supplement 6. Responses to IP_3 in various cell types.

Figure supplement 7. IP_3R is not essential for EL-Ca^{2+} refilling.

Figure supplement 8. TRPML1 releases Ca^{2+} from the EL-Ca^{2+} store in HeLa cells.

Figure supplement 9. ELGA is located to the endo-lysosome, distinct to the ER.

Supplementary Table 1. Colocalization of ELGA with organelle markers.

Supplementary Table 2. Super-resolution analysis of colocalization of ELGA with organelle markers**.**

Supplementary Movie 1. Localization of ELGA to punctate structures compatible with endo-lysosome.

Fig. S1

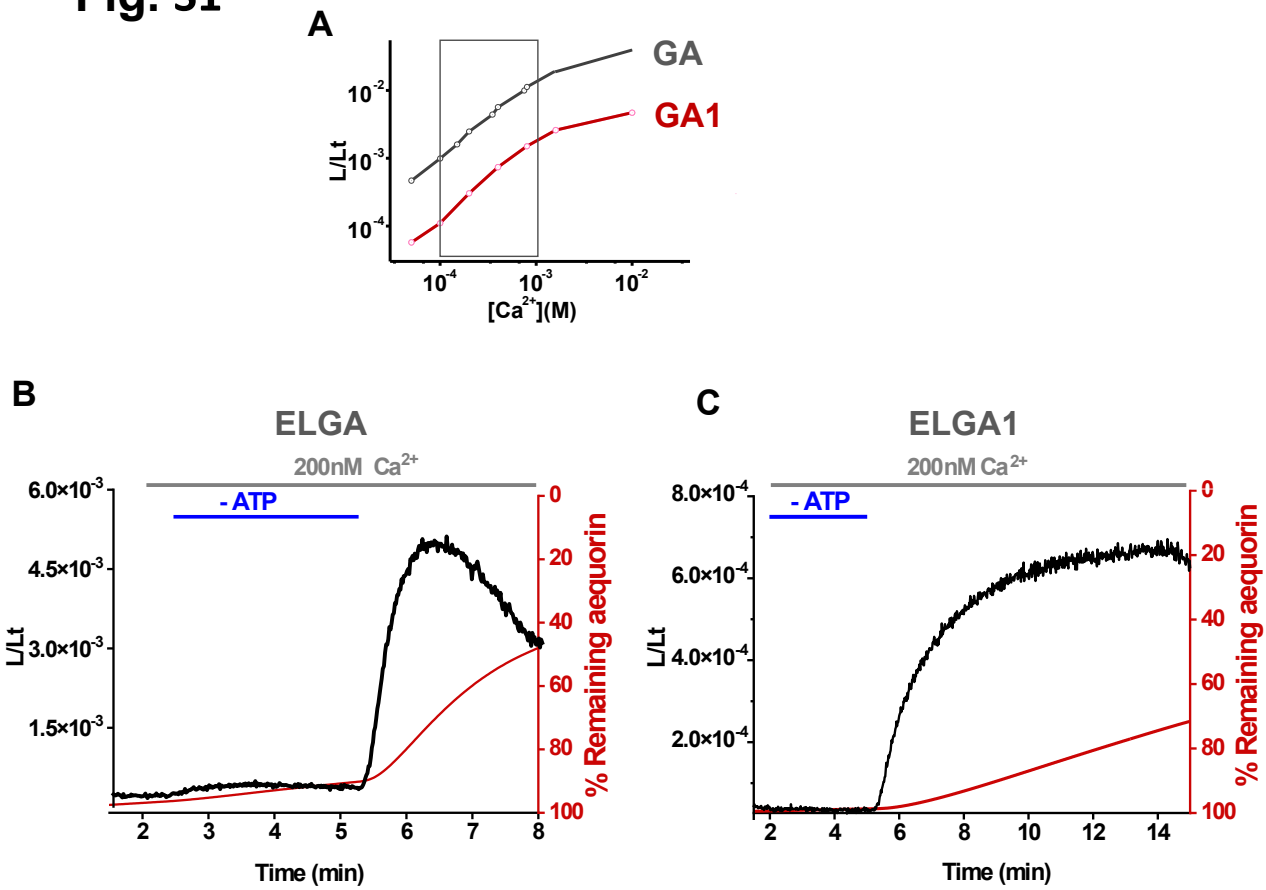

Figure supplement 1.

GA and GA1 bioluminescent Ca^{2+} sensors. (A) Ca^{2+} calibration of GA and GA1. The marked region is the range of [Ca^{2+}] expected in the endo-lysosome. **(B, C)** Comparison of emission (in L/Lt) and consumption (in % of the total) of luminescence in a representative experiment performed in transiently transfected HeLa cells with ELGA **(B)** or ELGA1 **(C),** both reconstituted with *n* coelenterazine. Permeabilized cells were perfused with an intracellular medium with 200 nM [Ca^{2+}] and without ATP (-ATP). Ca^{2+} uptake was triggered when ATP (1 mM) was reintroduced. Other experimental details as in Fig. 2. Each trace is representative of at least 4 independent transfections. Notice the stability of the ELGA1 signal at the steady-state (less than 5% aequorin consumed at min 8) in comparison with the ELGA signal that quickly declines due to the rapid consumption (~50% aequorin consumed at min 8).

Fig. S2

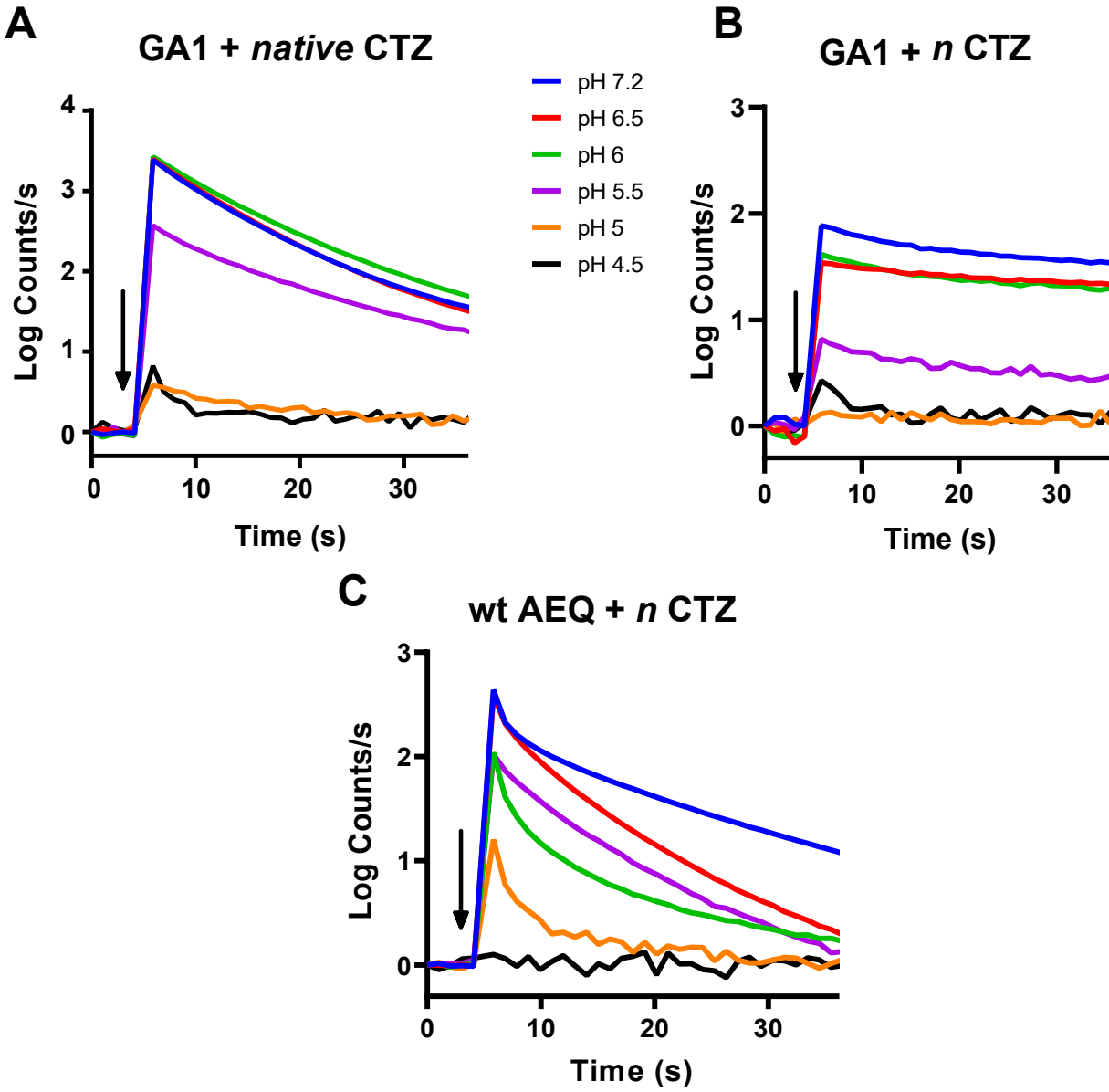

Figure supplement 2.

Effect of acidic pH on aequorin luminescence emission. *E.coli* recombinant GA1 with either native- (**A**) or *n*-coelenterazine (CTZ) (***B***) at the indicated pHs for 20 min and then subjected to luminescence emission assay triggered with 10 mM $CaCl_2$ (arrow) and measured at the same pH. Buffers used were: acetate for range 4.5-5.5 pH; Na-MOPS for 6 and 6.5 pH; and Na-Hepes for 7.2 pH. **(C)** *E.coli* recombinant wt-Aequorin reconstituted with *n*-coelenterazine. Each trace (A-C) is the value normalized with respect to its background emission before addition of calcium. Each trace is the average of 3-4 independent experiments. Other experimental details as described for Fig. 1E.

Fig. S3

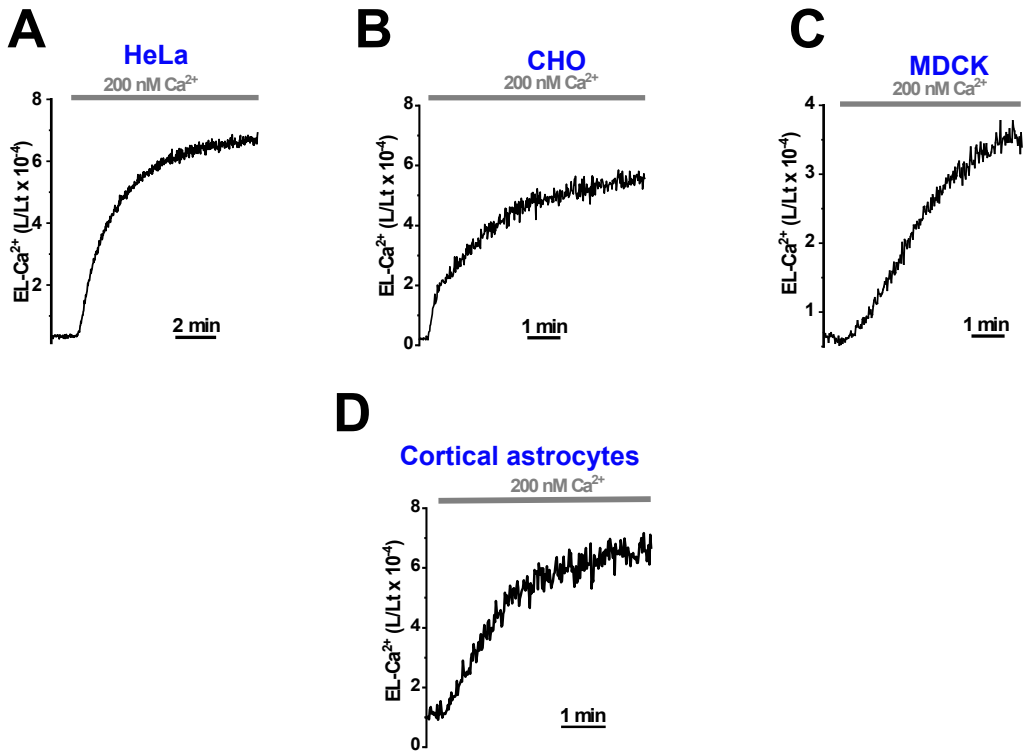

Figure supplement 3.

EL-Ca^{2+} dynamics in various cell types. (A) HeLa cells; **(B)** CHO cells; **(C)** MDCK cells; **(D)** mouse cortical astrocytes. All cell types expressed ELGA1 reconstituted with *n* coelenterazine. Cells were permeabilized in Ca^{2+}-free intracellular medium and then perfused 200 nM [Ca^{2+}] as indicated. For further details, refer to Figure 2A. Each trace is representative of at least 3 independent transfections.

Fig. S4

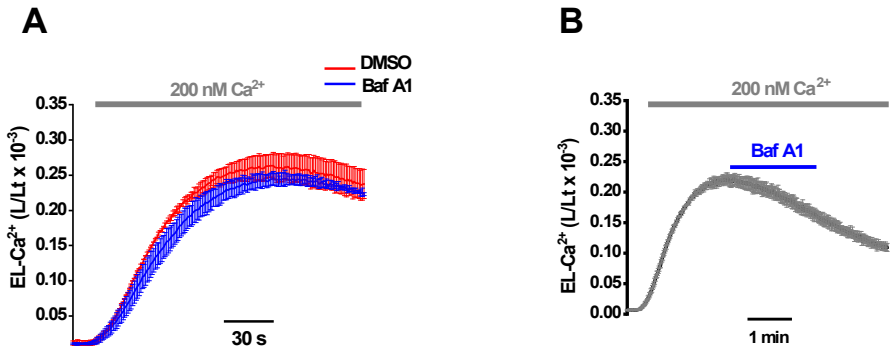

Figure supplement 4.

Effects of Bafilomycin A1 on the EL-Ca^{2+} dynamics. (A) ELGA transiently expressing HeLa cells were reconstituted with *n* coelenterazine together with Bafilomycin A1 (1 μM, blue trace) or DMSO (red trace) for 1h. Cells were permeabilized in Ca^{2+}-free intracellular medium and then perfused with 200 nM [Ca^{2+}], as indicated. **(B)** Acute application of Bafilomycin A1 (1 μM, 120s). Traces (A and B) are the mean ± S.E.M. of 6 experiments from, at least, 2 independent days.

Fig. S5

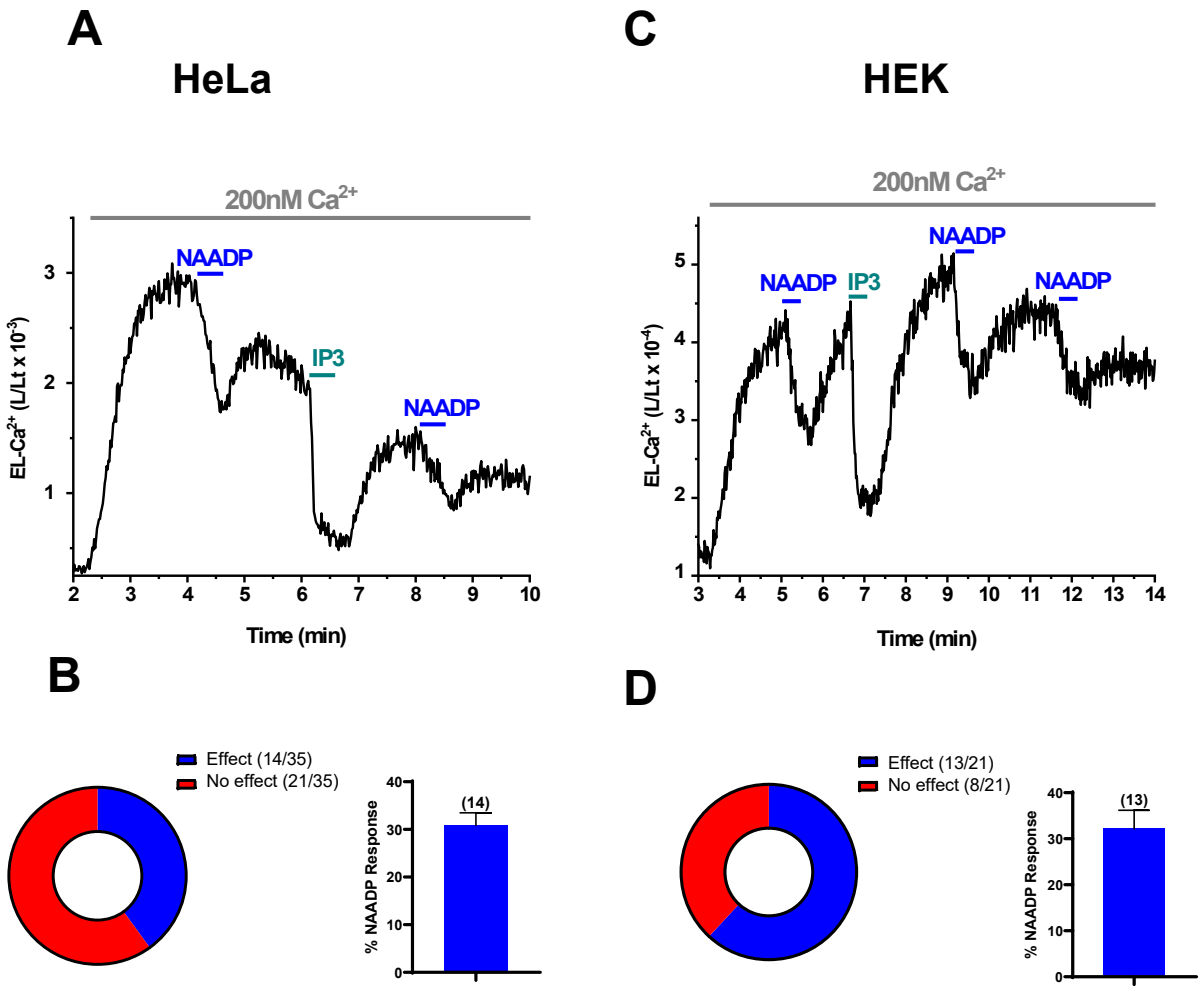

Figure supplement 5.

NAADP evoked Ca^{2+} release from the endo-lysosome. (A, C) Representative measurements of HeLa cells stably-expressing ELGA **(A)** or HEK293T cells transiently expressing ELGA **(B)** in which NAADP (100 nM) provoked an EL-Ca^{2+} release. IP_3 (2 μM) was also included for comparison. **(B, D)** Pie charts (left) show statistical quantifications of the all the experiments where NAADP response was tested in Hela (B) or Hek293T cells (D). Responses of NAADP-induced EL-Ca^{2+} release were shown in blue and no effect responses in red. Blue bars (right) show quantification of the NAADP release (mean ± S.E.M.) as the percentage of EL-total Ca^{2+} content at the steady-state of the number of independent experiments shown in parentheses.

Fig. S6

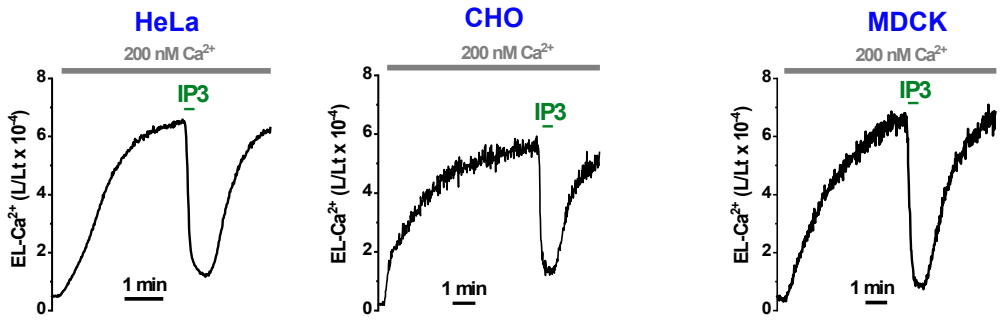

Figure supplement 6.

Responses to IP_3 in various cell types. Representative EL-Ca^{2+} release (in L/Lt ratio) upon application of IP_3 (2 μM) in HeLa, CHO or MDCK cells expressing ELGA1. Cells were permeabilized in Ca^{2+}-free intracellular medium, perfused with 200 nM [Ca^{2+}] and stimulated with IP_3 as indicated. Other experimental details as in Fig. 3A.

Fig. S7

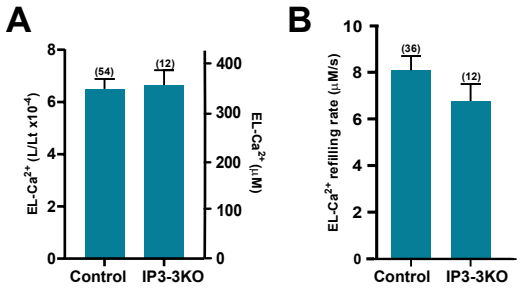

Figure supplement 7.

IP_3R is not essential for EL-Ca^{2+} refilling. Comparison of resting $[Ca^2]_{EL}$ **(A)** and EL-refilling Ca^{2+} rate **(B)** between control and IP_3R-3KO HEK cells**.** A Student's *t* test was applied. Values are expressed as mean ± S.E.M of the number of independent transfections in parentheses. No significant differences were observed.

Fig. S8

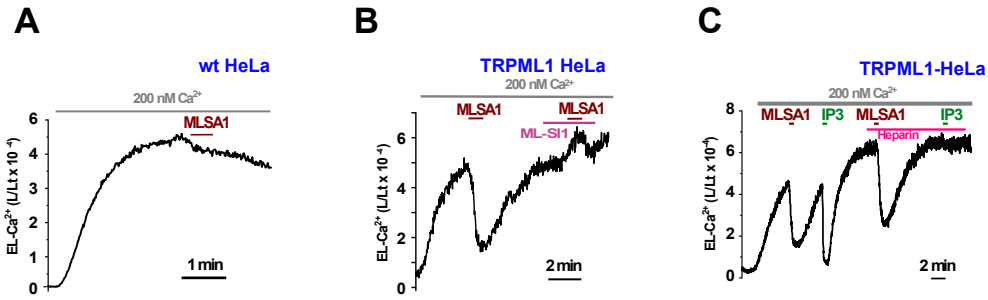

Figure supplement 8.

TRPML1 releases Ca^{2+} from the EL-Ca^{2+} store in HeLa cells. (A) ELGA expressing wt HeLa cells were challenged with ML-SA1 (20 µM, 30 s). **(B, C)** Similar to protocol in (A) but in transiently expressing-TRPML1 HeLa cells. The second application of ML-SA1 was performed in the presence of the TRPML1 inhibitor ML-SI1 (10 µM) (B). Comparison between the ML-SA1 and the IP_3 responses. Heparin (100 µg/mL) specifically blocked the IP3 response without affecting the MLSA1response (C).

Fig. S9

A

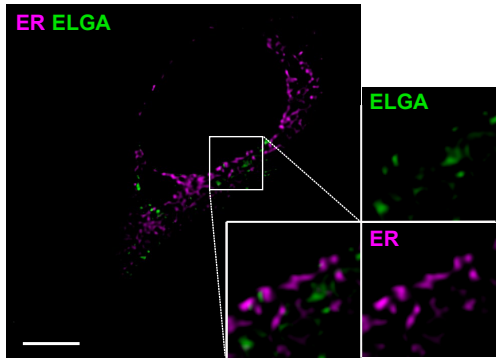

B

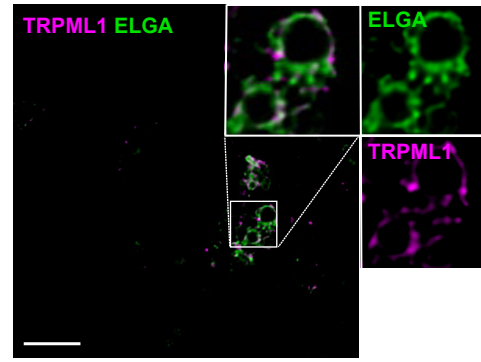

Figure supplement 9.

ELGA is located to the endo-lysosome, distinct to the ER. Detail of one Z- plane (1 µm) super-resolution images taken of HEK293T cells co-expressing ELGA (*green*) with either an ER marker (*magenta*)(**A);** or ELGA (*green*) with TRPML1 (*magenta*) (**B). (A)** Note that, in contrast to Figure 4M (maximal Z projection), no white puncta are visible. **(B)** Super-resolution images of two individual lysosomes in one Z-plane showing colocalization of ELGA and TRPML1. Scale bar for both images, 5 µm.

Figure 1- Supplement Table 1. Colocalization of ELGA with organelle markers.

Organelle marker	Pearson coefficient (r)	Mander´s coefficient M1 (ELGA/marker)	Mander´s coefficient M2 (marker/ ELGA/)	n
LAMP-2	0.60 ± 0.03	0.55 ± 0.06	0.45 ± 0.04	10
ER	0.42 ± 0.02	0.35 ± 0.03	0.12 ± 0.02	10
Early endosome (EE)	0.27 ± 0.03	0.13 ± 0.01	0.24 ± 0.03	10
Mitochondria (mt)	0.20 ± 0.03	0.29 ± 0.05	0.14 ± 0.02	12

ELGA expressing HEK293T were either immunostained with anti-LAMP2 antibody; cotransfected with er-Ruby-GCaMP210 (ER); immunostained with the anti-early endosome antigen 1 (EE); or immunostained with the anti-TOM20 antibody (mt). Pearson's (r) and Manders' (M1 and M2) correlation coefficients for colocalization of markers in confocal images of ***n*** number of cells from 3 independent experiments.

Figure 4- Supplement Table 2. Colocalization of ELGA with organelle markers

Organelle marker	Pearson coefficient (r)	Mander´s coefficient M1 (ELGA/marker)	Mander´s coefficient M2 (marker/ELGA/)	n
ER	0.28 ± 0.04	0.21 ± 0.04	0.03 ± 0.01	15
TRPML1	0.65 ± 0.03	0.75 ± 0.05	0.37 ± 0.02	20

ELGA expressing HEK293T were either cotransfected with er-targeted td-Tomato-Aequorin (ER) or with TRPML1-cherry. Super-resolution confocal images (0.38 µm) were analysed. Pearson's (r) and Manders' (M1 and M2) correlation coefficients for colocalization of markers. ***n*** indicates the number of images analysed from 3 (ER) or 4 (TRPML1) cells.